*Army Research Laboratory*

# Weather Effects on Target Acquisition Part I: Sensor Performance Model Infrared Algorithms

by
Richard C. Shirkey
Barbara J. Sauter

Computational and Information Sciences Directorate
Battlefield Environment Division

René V. Cormier
U.S. Air Force Research Laboratory
(Dynamics Research Corporation)

ARL-TR-821 July 2001

Approved for public release; distribution unlimited.

20010802 034

# NOTICES

## Disclaimers

The findings in this report are not to be construed as an official Department of the Army position, unless so designated by other authorized documents.

Citation of manufacturers' or trade names does not constitute an official endorsement or approval of the use thereof.

# REPORT DOCUMENTATION PAGE

*Form Approved*
*OMB No. 0704-0188*

Public reporting burden for this collection of information is estimated to average 1 hour per response, including the time for reviewing instructions, searching existing data sources, gathering and maintaining the data needed, and completing and viewing the collection information. Send comments regarding this burden estimate or any other aspect of this collection of information, including suggestions for reducing this burden, to Washington Headquarters Services, Directorate for Information Operations and Reports, 1215 Jefferson Davis Highway, Suite 1204, Arlington, VA 22202-4302, and to the Office of Management and Budget, Paperwork Reduction (0704-0188), Washington, DC 20503.

**1. AGENCY USE ONLY** *(Leave blank)*

**2. REPORT DATE**
July 2001

**3. REPORT TYPE AND DATES COVERED**
FINAL

**4. TITLE AND SUBTITLE**
Weather Effects on Target Acquisition Part I: Sensor Performance Model Infrared Algorithms

**5. FUNDING NUMBERS**

**6. AUTHOR(S)**
Richard C. Shirkey
Barbara J. Sauter
René V. Cormier, U.S. Air Force Research Laboratory, Dynamics Research Corporation

**7. PERFORMING ORGANIZATION NAME(S) AND ADDRESS(ES)**
U.S. Army Research Laboratory
Information Science and Technology Directorate
Battlefield Environment Division
ATTN: AMSRL-CI-EW
White Sands Missile Range, NM 88002-5501

**8. PERFORMING ORGANIZATION REPORT NUMBER**
ARL-TR-821

**9. SPONSORING/MONITORING AGENCY NAME(S) AND ADDRESS(ES)**
U.S. Army Research Laboratory
2800 Powder Mill Road
Adelphi, MD 20783-1145

**10. SPONSORING/ MONITORING AGENCY REPORT NUMBER**
ARL-TR-821

**11. SUPPLEMENTARY NOTES**

**12a. DISTRIBUTION/AVAILABILITY STATEMENT**
Approved for public release; distribution unlimited.

**12b. DISTRIBUTION CODE**
A

**13. ABSTRACT** *(Maximum 200 words)*

The U.S. Air Force, Navy, and Army are in the process of upgrading the Electro-Optical Tactical Decision Aid (EOTDA). The EOTDA has been used to predict the impact of weather and time of day on target acquisition. The upgraded program is called the Target Acquisition Weather Software (TAWS). New features of the TAWS will include: automated data access; upgraded path radiance routines; replacement of separate infrared (IR); television (TV) and night vision (NV) sensor performance models with Acquire; and a U.S. Army standard sensor performance model, which has become a standard in Department of Defense for IR, TV, and NV systems. To quantify the effects on predicted target acquisition range of upgrading the sensor performance model, a comparison of the TAWS Version 2 with Acquire has been undertaken. Weather effects on target acquisition are examined also in some detail.

**14. SUBJECT TERMS**
weather effects, target acquisition, Acquire, TAWS, clutter

**15. NUMBER OF PAGES**
64

**16. PRICE CODE**

| 17. SECURITY CLASSIFICATION OF REPORT | 18. SECURITY CLASSIFICATION OF THIS PAGE | 19. SECURITY CLASSIFICATION OF ABSTRACT | 20. LIMITATION OF ABSTRACT |
|---|---|---|---|
| UNCLASSIFIED | UNCLASSIFIED | UNCLASSIFIED | SAR |

NSN 7540-01-280-5500

Standard Form 298 (Rev. 2-89)
Prescribed by ANSI Std.Z39-18

## Acknowledgements

The authors would like to acknowledge the many and beneficial discussions with Dave Dixon, Training and Doctrine Command Analysis Center–White Sands Missile Range (TRAC–WSMR), John Mazz, Army Materiel Systems Analysis Agency (AMSAA), Melanie Gouveia, Logicon, and Dave Schmieder, Georgia Tech Research Institute (GTRI) that occurred during the course of this work. Their aid in providing information and tracking down documents concerning both the Acquire and TAWS sensor performance models was invaluable.

# Contents


**Preface** iii

**Acknowledgements** v

**Executive Summary** 1

**1. Introduction** 5

**2. Background** 7

2.1 Minimum Resolvable and Detectable Temperatures 7

2.2 Sensor Performance Models 8

2.2.1 Acquire SPM and Methodology 9

2.2.2 TAWS SPM and Methodology 14

2.2.2.1 Resolved Versus Unresolved Targets 16

2.2.2.2 Determination of SCR 17

2.2.3 Discussion 21

**3. Comparisons** 23

3.1 Scenarios 23

3.2 Model Runs 24

3.2.1 Characteristic Dimension 24

3.2.2 Sensor Curves 26

3.2.3 Aspect Ratios 26

3.2.4 Backgrounds 27

3.2.5 Clutter 28

3.3 Results 29

3.3.1 Clutter/Complexity Effects 30

3.3.2 Weather Effects 33

3.3.2.1 Visibility 33

3.3.2.2 Relative Humidity 33

3.3.2.3 Sky Cover 36

3.3.2.4 Fog and Precipitation 37

**4. Conclusions** 39

**References** 41

**Acronyms** 45

**Distribution** 47

**Figures**

1. Equivalent bar pattern 10

2. Target-acquisition methodology 11

3a. Initial clutter temperature algorithm 20

3b. Current clutter temperature algorithm 20

4. Probability of detection versus resolution for 50 percent acquisition level using the TAWS and Acquire algorithms 21

5a. T–80B 25

5b. T–80U 25

6. Comparison of the TAWS and Acquire MRT curves 26

7. Acquire versus the TAWS clutter comparison 28

8. The TAWS versus Acquire-detection ranges at 50 percent probability of detection 29

9. Scene complexity effects on target-detection ranges 31

10. Visibility impacts on the TAWS-detection ranges 35

11. Relative humidity impacts on the TAWS-detection ranges 35

12. Sky cover impacts on the TAWS-detection ranges 37

13. Fog impacts on the TAWS-detection ranges 38

14. Precipitation impacts on the TAWS-detection ranges 38

**Tables**

1. $N_{50}$ as a function of Acquire version 14

2. Summary of detection methods 17

3. Clutter temperature $C_T$ values 18

4. Algorithm for determining $S_c$ 19

5. Initial TAWS implementation of $C_T$ algorithm 19

6. Current TAWS implementation of $C_T$ algorithm 20

7. Weather conditions used in the study 23

8. Problems between TAWS and Acquire algorithms and their resolution 24

9. T-80 dimensions 25

10. Impact of a second background on detection range 32

11. Detection ranges as a function of various weather 34

# Executive Summary

## Overview

The range a target can be detected on the battlefield is a valuable piece of information for the battlefield commander. Detection and recognition ranges depend upon the target and background characteristics, atmospheric propagation, and sensor performance. Weather tactical decision aids provide information on sensor performance under adverse weather conditions.

The Target Acquisition Weather Software (TAWS) is an updated version of the U.S. Air Force Electro–Optical Tactical Decision Aid. The TAWS provides U.S. Air Force, Navy and Army mission planners and warfighters with appropriate information for optimal sensor and/or weapon systems selection, acquisition range determination, and mission routing under degraded weather conditions. The TAWS was originally constructed to predict detection and lock-on ranges only. Because the U.S. Army extensively makes use of recognition and identification ranges, methodologies for adding this information to the TAWS were examined. The leading algorithm, and thus, a contender for the replacement of the current algorithm, is Acquire.

Physics-based Tactical Decision Aids (TDA)s, such as TAWS, employ physics calculations that have their basis in theory or measurements. Thus, a physics-based TDA employs routines and physics that allow it to ascertain the probability of detecting a given target at a given range under existing or predicted weather conditions. The effects and methodology for determination of the range a target is detected under adverse weather conditions at infrared (IR) wavelengths is the subject of this report. The sensor performance model Acquire and the senor performance model in TAWS both use what is known as the equivalent bar pattern approach; however, the underlying assumptions of each algorithm are considerably different. The purpose of this report is to show the differences between these two methodologies and to examine weather effects on target-acquisition ranges.

## Background

Typical performance prediction models for resolved targets (a target is considered to be resolved when the target-angular subtense nominally exceeds the sensor's angular subtense in both vertical and horizontal dimensions at the range of interest) treat the target with the bar/target equivalency criteria and the sensor with the minimum resolvable temperature (MRT) function. Bar- and target-signal equivalency is established by equating the bar pattern temperature difference to the target average temperature difference. The detection range is sharply bounded in that it can never exceed the range at which the target ceases to be resolved, that is the (detection) range ≈ target size/resolution.

Models for predicting the detection range of unresolved targets typically rely strictly on target-signal strength for detection. These models typically abandon both the bar- and target-equivalency criteria and the MRT approach. Unresolved target models are often called "hot spot" or "star detection" models because they rely on high-apparent contrast for detection. The "target" is a square or circle with dimensions matched to the high temperature target area of interest. This target spot detection methodology applies to cases the target is viewed against a uniform background, and detection occurs when the signal-to-noise ratio on the display element that subtends the target exceeds that of the background. The methodology for spot detection applies only to the detection of the target (its discrimination from the background), and not to levels of target discrimination. The sensor function is the minimum detectable temperature (MDT).

The MDT is only appropriate for targets against a uniform or unstructured background, for example, aircraft against a clear or overcast sky or vehicles in a desert background. Searching for tanks against a varied terrain background requires the MRT approach. Additionally, the MDT approach only represents detection whereas the MRT approach, which may also be used for detection, is required for target recognition and identification.

Target detection, recognition, and identification methodology applies to situations in which the target is embedded in a non-uniform or cluttered background and it is necessary to separate the target characteristics from the background. The target discrimination MRT methodology, based on the Johnson cycle criteria in Acquire and Schmieder's criteria in TAWS, can be used for the prediction of target-acquisition range at

discrimination levels of detection, recognition, and identification. Both the TAWS and Acquire can use MDT to predict detection range also.

The TAWS currently uses Schmieder's work implemented to predict detection; higher discrimination levels, such as recognition and identification, are not included. Because Acquire is currently both the U.S. Army and Air Force standard for target acquisition, and it predicts ranges for discrimination levels of detection, recognition, and identification, it was decided to replace the current sensor performance model (SPM) resident in the TAWS with Acquire. However, this replacement raises the question of what differences may arise due to different methodologies between the SPMs in the TAWS and Acquire. To answer this question for IR sensors, a comparison of static target discrimination methodologies and the resultant target-acquisition ranges produced by the TAWS and Acquire was undertaken. It should be noted that this comparison in no way should be construed as a validation of the target-acquisition ranges. Rather we are examining what, if any, differences that arise due to the underlying SPMs and the methods that they implemented.

To compare these two complex target-acquisition models required standardization of as many parameters as possible. To accomplish this, one weather scenario was used in conjunction with one sensor and target, both with fixed orientations. Thus, a winter scenario was chosen and examined using an exercised T-80 Soviet main battle tank against two backgrounds (vegetation and snow) at IR wavelengths. The sensor and tank were aligned such that the sensor always had a frontal view of the tank; the sensor height was fixed at 300 ft facing north. The date was fixed at 21 December at a local time of 12N; the location was fixed at latitude of 37°32' N, longitude of 127°00' E (Seoul, South Korea). The weather conditions included clear skies with varying visibility and relative humidity and overcast skies with varying visibility and relative humidity. Additional cases were run including light/heavy fog conditions, snow, drizzle, and rain.

## Conclusions

The SPM in the TAWS is based on Schmieder's image-based work and thus requires additional algorithms to determine the effects of clutter in the scene; these algorithms are not necessarily intuitive. Since Acquire's target transform probability function and Schmieder's detection probability as a function of resolution, agree reasonably well under

moderate clutter conditions, and because Acquire is an industry, U.S. Army and Air Force standard, it was decided to replace the current SPM with Acquire. Clutter levels can be accommodated in Acquire by varying the $N_{50}$ parameter.

The incorporation of the Acquire SPM into the TAWS is scheduled for the TAWS Version 3, which will be released for use in 2001. The comparisons shown here, of target-acquisition range output from the current version of TAWS with output from Acquire, provide positive feedback on the benefits of this enhancement to TAWS, while maintaining existing interfaces and providing comparable target-detection range predictions. The primary benefit of this enhancement will be the ability to specify target acquisition discrimination levels, including detection, recognition, and identification.

Because the cases examined in this report are limited to a winter scenario in Korea, specific quantitative results of the selected weather parameters' impacts on target-detection range cannot be generalized to all situations. However, these cases do highlight the importance of considering accurate atmospheric conditions in target-acquisition predictions. Results show a smaller weather impact to Acquire detection ranges than predicted using the current TAWS SPM under conditions of fog or precipitation.

# 1. Introduction

The range a target can be detected on the battlefield is a valuable piece of information for the battlefield commander. Detection and recognition ranges depend upon the target and background characteristics, atmospheric propagation, and sensor performance. Weather tactical decision aids (TDA)s, which provide information on sensor performance under adverse weather conditions, come in two forms:

1. rule based and
2. physics based.

Rule-based TDAs, such as the U.S. Army's Integrated Weather Effects Decision Aid (IWEDA) [1] are constructed using observed impacts that have been collected from field manuals, training centers and schools, and subject matter experts.

Physics-based TDAs, such as the Target Acquisition Weather Software (TAWS) [2] and Acquire [3], employ physics calculations that have their basis in theory or measurements. Thus, a physics-based TDA employs routines and physics that allow it to ascertain the probability of detecting a given target at a given range under existing or predicted weather conditions. The effects and methodology for determination of the range at which a target is detected under adverse weather conditions at IR wavelengths is the subject of this report. The TAWS and Acquire both use what is known as the equivalent bar pattern approach; however, the underlying assumptions of each algorithm are considerably different. The purpose of this report is to show on the differences between these two methodologies and to examine weather effects on target-acquisition ranges.

# 2. Background

## 2.1 Minimum Resolvable and Detectable Temperatures

Typical performance prediction models for resolved targets (a target is considered to be resolved when the target-angular subtense nominally exceeds the sensor's angular subtense in both vertical and horizontal dimensions at the range of interest) treat the target with the bar- and target-equivalency criteria and the sensor with the minimum resolvable temperature (MRT) function. This methodology assumes that resolved targets are detected, based on observer pattern recognition. Signal strength only needs to be sufficient in order to define the pattern. The signal is typically defined as the temperature difference between the average temperature of the target and a uniform background temperature as seen by the sensor. Bar- and target-signal equivalency is established by equating the bar pattern temperature difference to the target average temperature difference. The detection range is sharply bounded so that it can never exceed the range at which the target ceases to be resolved, that is the (detection) range $\approx$ target size/resolution. This is the maximum range at which a periodic target can be faithfully reproduced; thus a target is considered unresolved if the projected sensor instantaneous field of view (IFOV) is greater than 80 percent of the target's critical dimension. The percentage is taken to be 80 percent because other sensor apertures, in addition to the detector IFOV, cause the effective system IFOV to be slightly larger.

Models for predicting the detection range of unresolved targets typically rely strictly on target-signal strength for detection. These models typically abandon both the bar- and target-equivalency criteria and the MRT approach. Unresolved target models are often called *hot spot* or *star detection* models because they rely on high apparent contrast for detection. The *target* is a square or circle with dimensions matched to the high temperature target area of interest. This target spot detection methodology applies to cases in which the target is viewed against a uniform background, and detection occurs when the signal-to-noise ratio on the display element that subtends the target exceeds that of the background. That is, a sufficient amount of target energy reaches a detector element to create a *hot spot* on the system display. (For this reason, spot detection is also referred to as *star* detection.) The

methodology for spot detection applies only to the detection of the target (its discrimination from the background), and not to levels of target discrimination. The sensor function is the Minimum Detectable Temperature (MDT). Detection range predictions are not sharply bounded with this unresolved target methodology since target-signal strength does not abruptly disappear after becoming unresolved.

The MDT is only appropriate for targets against a uniform or unstructured background; for example, aircraft against a clear or overcast sky or vehicles in a desert background. Searching for tanks against a varied terrain background requires the MRT approach. Additionally, the MDT approach only represents detection whereas the MRT approach, which may also be used for detection, is required for target recognition and identification. If a target is hot enough, the MDT approach predicts target detection even though the target may be smaller than a forward-looking infrared (FLIR) detector element. For all practical purposes, the MDT approach is not used in the Army's combat simulations since recognition or identification is required before firing on a target. It should also be noted that in a cluttered environment the target would not be the only hot spot.

## 2.2 Sensor Performance Models

Target detection, recognition, and identification methodology applies to situations in which the target is embedded in a non-uniform or cluttered background and it is necessary to separate the target characteristics from the background. The target discrimination MRT methodology, based on the Johnson cycle criteria [4] in Acquire and Schmieder's criteria [5,6] in the TAWS, can be used for the prediction of target-acquisition range at discrimination levels of detection, recognition, and identification. Both the TAWS and Acquire can use MDT to predict detection range also.

Acquire, developed by the U.S. Army Night Vision and Electronic Sensors Directorate (NVESD), is an analytical model that predicts target-detection and discrimination-range performance for systems that image in the visible, near-IR, and IR-spectral bands. Ranges and probabilities predicted by the model represent the expected performance of an ensemble of trained military observers with respect to an average target having a specified signature and size.

The U.S. Air Force Research Laboratory's (AFRL) Electro-Optical Tactical Decision Aid (EOTDA) [7] was developed to provide the user with a single piece of software to evaluate the combined effects of target-to-background contrast, atmospheric transmission, and sensor performance on the range at which a target can be detected by an imaging device. The model treats detection by television, image intensifiers, and thermal imaging devices. The TAWS, a Tri-Service program, is an upgrade of the EOTDA.

The TAWS currently uses Schmieder's work implemented to predict detection; higher discrimination levels, such as recognition, and identification, are not included. Because Acquire is currently both the Army standard [8] and a U.S. Air Force standard for target acquisition, and because it predicts ranges for discrimination levels of detection, recognition and identification, it was decided to replace the current sensor performance model (SPM) resident in the TAWS with Acquire. However, this replacement raises the question of what differences may arise due to different methodologies between the SPMs in the TAWS and Acquire. To answer this question for IR sensors, a comparison of static target-discrimination methodologies and the resultant target-acquisition ranges produced by the TAWS and Acquire was undertaken. It should be noted that this comparison in no way should be construed as a validation of the target-acquisition ranges per se. Rather we are examining what, if any, differences that arise due to the underlying SPMs and the methods that were implemented.

### 2.2.1 Acquire SPM and Methodology

During the 1950s, the military developed electro-optical image intensifiers, which provided enhanced visual surveillance capabilities under conditions of limited visibility. The complexity of these intensifiers and associated target-acquisition systems required a methodology for evaluating performance characteristics. John Johnson, of the then U.S. Army Engineer Research and Development Laboratories (ERDL) (currently NVESD), presented results of experiments with human observers conducted at ERDL to determine the resolution required of a system to perform certain target-interpretation processes such as target detection and recognition. He referred to these as *decision responses* and said that the processes were dependent upon the characteristics of the optical message, the properties of the intensifier device, and the physiological response of the human readout processes. Through a series of experiments using trained observers looking at targets and bar resolution diagrams, Johnson [4] developed a method relating the *decision*

*response* to the number of bars (line pairs) normalized to the shortest target dimension that an observer needed to see to make a decision (detection, recognition, etc.).

The methodology developed by Johnson was simple and straightforward. In the laboratory, scale models of various military targets were moved to a distance where they could just be detected as viewed by an observer through an image intensifier. Bar charts, with the same contrast as the scale models, were then placed in the observer's field of view at the same range as the target. The spatial frequency (line pairs) resolved by the observer was then determined as a function of contrast. This same methodology was used for determining the line pairs required by the observers to recognize the object seen as a tank. The spatial frequency of the pattern was specified in terms of the number of lines in the pattern subtended by the object's minimum dimension as illustrated in figure 1.

Figure 1 shows three bars across the tank's shortest dimension as seen by an observer; this is the criterion Johnson used for recognizing that the object was a tank. Further, Johnson found that the normalized line-pair resolution required for a particular "decision response" was nearly constant for the group of nine military targets he employed. In the case of target detection, that was 1.0-line pairs per shortest target dimension. These normalized (to the shortest target dimension) line pair values required for a *decision* were found to be independent of contrast and scene signal to noise ratio as long as the contrast on the bar chart was the same as the target contrast. The results showed that decision levels for military targets may be considered equivalent to bar patterns of appropriate spatial frequencies.

**Figure 1. Equivalent bar pattern.**

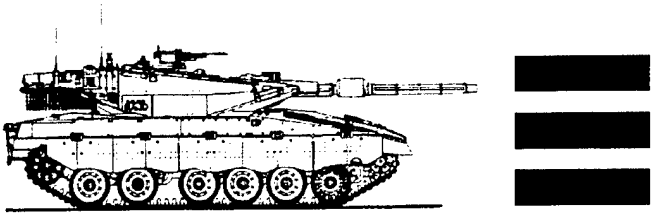

This methodology, which provided target-discrimination criteria based upon resolution, gained widespread acceptance within the industry and became the accepted criteria for performance measurement of optical systems. These criteria were referred to as the Johnson Criteria or equivalent bar pattern approach.

In 1974, 16 years after publishing his original paper, Johnson modified his original work and extended it to cover IR systems [9]. This paper emphasized that the values for the various decision levels are representative values, essentially average values required for 50 percent probability, and must not be construed as rigid or optimum values for specific targets and target-aspect views. The values associated with the various decision levels remained the same, (e.g., 1.0 line pairs for detection) except for recognition, which changed slightly. This paper also recommended and provided procedures for using the concept of MRT for thermal sensors. Johnson's methodology is schematically represented in figure 2. [10]

**Figure 2. Target-acquisition methodology.**

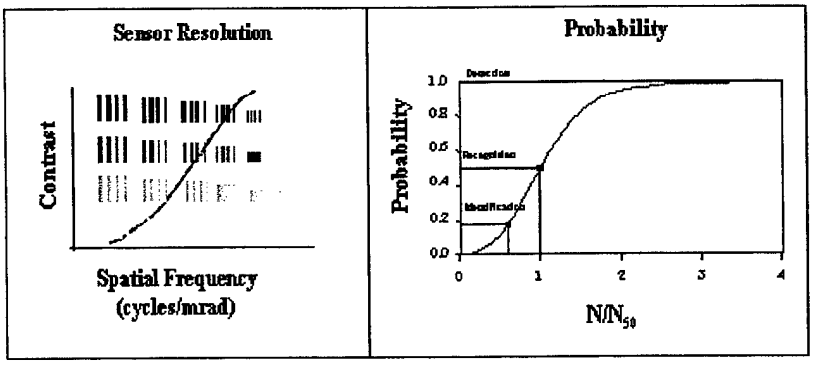


The MRT is defined as the temperature difference between a uniform background and the bars of a four-bar pattern, each bar having a 7:1 aspect ratio (so the overall pattern will be a square), which is required by a trained observer to just resolve all four bars when viewing the pattern through an imager. [11] The left side of the figure shows the resolvable temperature difference (contrast) versus the maximum resolvable bar pattern (spatial frequency) as a function of contrast. For a specific target-contrast level, the maximum resolvable spatial frequency is the highest spatial frequency at which a human observer can still recognize the four distinct bars and not one or two blobs. Thus, the temperature difference required to resolve the four bars increase, as the bars get smaller. This maximum resolvable spatial frequency is a

function of contrast (visual or thermal) and is the minimum resolvable contrast (MRC) in the visual or MRT difference curve in the thermal. In the figure, the bars represent the generic formulation, whereas the solid line would represent the target contrast and sensor resolution for a specific sensor. With knowledge of the target's contrast ($\Delta T$ in the IR), critical dimension, range, and the atmospheric attenuation, the number of resolvable cycles, N, across the target's critical dimension can be determined by

$$N = f_x \frac{H_{targ}}{R} , \tag{1}$$

where $f_x$ is the maximum resolvable spatial frequency of the sensor (in cy/mr) at the apparent $\Delta T_a$ (usually in °K), $H_{targ}$ is the target-critical dimension (in meters) and R is the range (in kilometers). The apparent thermal contrast is determined by

$$\Delta T_a = \Delta T \, T(R) , \tag{2}$$

where $T(R)$ is the atmospheric transmission. Under the assumption of a homogeneous atmospheric path the transmission may be found using Beer's law

$$T(R) = e^{-\beta R} \tag{3}$$

where $\beta$ is the atmospheric extinction coefficient determined from an atmospheric propagation code [12,13]. We now need a way to correlate N with the discrimination level: detection, recognition, and identification. Johnson did this by establishing the so-called target transform probability function (TTPF). [9] The TTPF, shown in the right-hand section of figure 2, was derived from laboratory psychophysical experiments in which the ability of observers to perform a particular discrimination task as a function of resolvable cycles across the target-minimum dimension was measured. For a given discrimination task, the TTPF represents the 50-percent point, referred to as $N_{50}$, as determined from this ensemble of

range. Thus, if the range is unknown, but information is available about the target-critical dimension, the target/background $\Delta T$, and the sensor response curve, then a solution can be found through iteration for the range at a predetermined $P_d$.

As FLIRs advanced from first to second generation, their resolution increased so that there was nearly equal resolution along the scan direction and perpendicular to it. This, in part, necessitated a change in the original one-dimensional (1D) version of Acquire. An updated version of Acquire, discussed in detail in reference 11, was issued in June 1990. The model update consisted of two parts:

1. FLIR90, which predicts laboratory measures and
2. a two dimensional (2D) version of Acquire, which predicts field performance.

In FLIR90, predicted or measured horizontal and vertical MRTs are averaged at a particular temperature using

$$f_{eff} = (f_x * f_y)^{1/2}. \qquad (4)*$$

This effective spatial frequency applies to the effective MRT used along with modified values of $N_{50}$ for the different discrimination tasks to predict range performance. The $N_{50}$ values for 1D or 2D are presented in table 1. The $N_{50}$ for a particular task, using the more recent 2D version of the model, is found by multiplying the original 1D $N_{50}$ values by 0.75. The amount of shift was determined by requiring the range predictions for the 2D model to correctly predict the results of field tests, which served as validation for the original (1D) model. The discrimination levels in figure 2 are for second generation FLIRs. As an example, if we have a target with a critical dimension of 3 m at a range of 3 km, with an apparent contrast that would give a maximum resolvable frequency of 3 cycles/mrad, this would lead to a probability of recognition, for a second generation FLIR, of 50 percent; with a first generation FLIR, this would lead to a probability of recognition of 25 percent.

---

* *The discussion in this paragraph relies heavily on reference 11.*

apparent contrast that would give a maximum resolvable frequency of 3 cycles/mrad, this would lead to a probability of recognition, for a second generation FLIR, of 50 percent; with a first generation FLIR, this would lead to a probability of recognition of 25 percent.

**Table 1. $N_{50}$ as a function of the Acquire version**

| | Acquire version | |
|---|---|---|
| | 1D | 2D |
| Detection | 1.0 | .75 |
| Recognition | 4.0 | 3.0 |
| Identification | 8.0 | 6.0 |

### 2.2.2 TAWS SPM and Methodology

The TAWS SPM is derived from work done in the 1980s at the U.S. Air Force Avionics Laboratory (now part of AFRL), which led to the development of a "research grade" TDA. The main difference between the TAWS and the Avionics research grade code lies primarily in the underlying thermal model, the Thermal Contrast Model 2–TCM2, with TAWS using a scaled-down version of that model. The SPM resident in TAWS uses the equivalent bar-chart approach but differs from Acquire by directly incorporating clutter effects for 50 percent probability of acquisition. The TAWS predicts lock-on range based on signal-to-noise ratio thresholds, hot spot detection based on MDT methodology, and discrimination detection range based on MRT methodology. Thus, all other parameters being equal, the TAWS detection ranges should be approximately equal to those predicted by Acquire at the 50 percent probability of detection level for moderate clutter (see discussion below). Clutter is automatically computed, based on an empirical algorithm [14], and is a strong factor in determination of the number of cycles on target.

During the 1980s, Dave Schmieder at the GTRI examined the effect of clutter on target detection. [5,6] He found that the amount and nature of background clutter had a significant impact on the probability of target detection. Schmieder first looked at scene radiance standard deviation as a clutter measure. However, this measure had the deficiency of giving large clutter values to relatively uncluttered scenes when those scenes possessed several intensity modes. Moreover, this definition, like many other amplitude measures [5], lacked a weighting factor based on target size. Both amplitude and target size measures appeared to be required to

predict observed trends. Since existing definitions appeared inappropriate, Schmieder redefined the term. The clutter definition he used was a scene radiance standard deviation computed by averaging the radiance variances of contiguous scene cells over the whole scene and taking the square root of the result. This is formulated as

$$clutter = [\sum_{1}^{N} \sigma_i^2 / N]^{1/2} , \tag{5}$$

where $\sigma_i$ is the radiance standard deviation for the $i^{th}$ cell and N is the number of contiguous cells in the scene. This definition implicitly included both target size and intensity measures and produced higher values for scenes that looked more complex and cluttered. It also avoided yielding a large clutter value for relatively uncluttered scenes that still contained variations in intensity. Additionally, it accounted for clutter object sizes close to the target size weighing more in the clutter calculation. However, as with other definitions of clutter, this definition introduces its own set of problems. Scene imagery is required to adequately determine $\sigma_i$ and eq (5) is not scale invariant but depends on the cell size selected for calculation. Schmieder took the cell size to be square in shape with side dimensions of approximately twice the target height. However, if the scene under examination contains more than one type of target (man, tank, bridge, etc.) the cell size must be redefined for each target examined, resulting in different values for $\sigma_i$ and N.

Based upon this definition, Schmieder performed experiments with observers which showed that clutter could be categorized according to the signal-to-clutter ratio (SCR) where the signal was the temperature difference between the maximum/minimum target temperature as seen by a sensor and the background temperature where the clutter was defined as above. Schmieder found that high clutter exhibited a SCR of $< 1$, moderate clutter an SCR of 1 to 10, low clutter an SCR $> 10$ and $< 40$, and no clutter effects could be assumed if the SCR $\geq 40$. Furthermore, Schmieder's data showed that for a detection probability of 50 percent, the number of cycles (line pairs) required for detection of a target varied between 0.5 for low clutter to 2.5 for high clutter, with moderate clutter requiring approximately 1.0 cycle.

Schmieder concluded that acquisition levels are a strong function of clutter as well as resolution and that range prediction models must include clutter effects. Because the number of line pairs per target-angular subtense necessary for detection is inversely proportional to detection range, changes in SCR can be expected to significantly alter target-detection range predictions.

The TAWS detection methodology uses Schmieder's SCR algorithm at the 50 percent probability of detection level to determine whether MRT or MDT formalization should be used and to calculate target-acquisition ranges. The SCR may be thought of as the ratio of hot/cold spot $\Delta T_T$ (i.e., maximum/minimum target temperature – background mean temperature) to clutter equivalent temperature ($C_T$), thus

$$SCR = \Delta T_T / C_T. \tag{6}$$

The value of $C_T$ is determined by the IR scene complexity (a measure of the number of objects in the scene competing with the target) in conjunction with the background scene contrast ($S_C$) in the target's vicinity. Since detection methodology and acquisition range both depend upon SCR (discussed in some detail below).

The TAWS determination of acquisition range is fixed at 50 percent probability of detection. Thus, as mentioned above in the section on Acquire MRT methodology, a solution for the range can be found if the target's critical dimension, target and background temperatures, and MRT sensor curve are all known. While TAWS uses this methodology, there are significant differences from Acquire—most notably in the determination of the number of line pairs on target, N.

#### 2.2.2.1 Resolved Versus Unresolved Targets

Whether the TAWS computes the detection range via MRT or MDT methodology depends on whether the target is resolved or unresolved at a given sensor to target range and the SCR at that range.

For resolved targets, if the SCR > 40, indicating little or no clutter, MDT is used with the target contrast based on the temperature difference between the hottest (or coldest) facet of the target seen by the sensor and a given background; this is referred to as $\Delta T_{MAX}$. Even though the target is resolved, Schmieder did not recommend using MRT because he felt that with such a high signal to clutter ($\geq$ 40), it does not matter if the target is resolved or not, and MDT (hot/cold spot) detection would give a longer detection range than MRT. If the SCR is < 40, MRT is used with the target contrast, $\Delta T_{AVG}$, being the difference of the average temperature of the target facets seen by the sensor and the background temperature.

If the target is unresolved at a given range, it is either detected with the MDT methodology or is not detectable at all. If the unresolved target is detectable using MDT, then SCR ≥ 40. In that case, $\Delta T_{MAX}$ is used for the target and background contrast. If SCR < 40, and the target is unresolved, then the clutter is too high, and no detection occurs at this range and the range must be decreased for detection to occur. These results are summarized in table 2.

**Table 2. Summary of detection methods**

| SCR | Line pairs on target | Method |
|---|---|---|
| < 1 | 2.5 | MRT |
| ≤ 1 < 10 ≤ | 1.0 | MRT |
| 10 < 40 | 0.5 | MRT |
| ≥ 40 | - | MDT |

For calculating the SCR in the above procedures, Schmieder recommended using the signal $\Delta T_{MAX}$ rather than $\Delta T_{AVG}$, for the reason that in his 1982 SCR study [6] the signal component was defined as $\Delta T_{MAX}$ rather than $\Delta T_{AVG}$.

2.2.2.2 Determination of SCR

In the absence of actual imagery of the target area, Schmieder estimated clutter from a combination of scene complexity and $S_c$. We present his methodology in some detail below.

Schmieder's SCR algorithm affects the acquisition range by modifying the number of line pairs (N) on target. At 50 percent probability of detection, Schmieder's results can be formulated as [15]

$$N = \frac{1.64}{(\log(SCR) + 1.2)^{1.51}} \frac{H_{targ}}{R} \tag{7}$$

for SCR ≥ 0.1. The TAWS uses the target height for the target-critical dimension, $H_{targ}$. In order to determine SCR from eq (6) both the target contrast ($\Delta T_T$) and the clutter temperature, $C_T$ must be known. $C_T$, in turn, requires knowledge of both scene contrast and scene complexity. Because the TAWS does not produce or use target- and background-scene images, it cannot compute clutter as originally defined by Schmieder. To rectify this problem, Schmieder [16] recommended that clutter be computed based on $C_T$. He assumed that on the average, the target contrast, $\Delta T_T$, which represents the temperature difference between target and background, would be equal to 2 °C. Schmieder then used eq (6), with the average $\Delta T_T$ 2 °C, coupled with SCRs of 40, 10, 4, and 1, representing clutter states of none, low, moderate, and high respectively, to determine values for $C_T$. Schmieder states [16], "Clearly, other assumptions of target signal and SCR would lead to other associated values. The values shown (in table 3) are used as a starting point to be used until the results of further research can yield a better basis for these choices."

A method for relating scene contrast ($S_C$) to the clutter levels is needed. Schmieder chose [17] $S_C$ ranges of 0 to 1, 1 to 2, 2 to 4, and > 4 to correspond to the clutter levels of none, low, moderate, and high, respectively. These quantities (SCR, $C_T$, $S_C$) and their relation to clutter level are summarized in table 3.

**Table 3. Clutter temperature $C_T$ values**

| Clutter level | SCR | $C_T$ (degrees C) | $S_C$ range (degrees C) |
|---|---|---|---|
| none | 40 | .05 | ≤ 1.0 |
| low | 10 | .2 | > 1.0 - ≤ 2.0 |
| moderate | 4 | .5 | > 2.0 - ≤ 4.0 |
| high | 1 | 2 | > 4.0 |

To obviate the need for the user to select a clutter level, the TAWS implemented Schmieder's algorithms to determine CT based on a user input of IR-scene complexity and a calculation of scene-thermal contrast by the TAWS IR model. [18] The algorithm for determination of $S_C$ as found in TAWS, is presented in table 4. In this table, $T_B$ is a background temperature and the subscripts 1 and 2, H and L refer to the first and second, high and low background temperatures, respectively. Table 5 and figure 3a show the original implementation.

Table 4. Algorithm for determining $S_C$

| Number of backgrounds | $S_C$ value (degrees C) |
|---|---|
| 1 | 0.5 |
| 2 | $\lvert T_{B1} - T_{B2} \rvert$ |
| 3 | $T_{BH} - T_{BL}$ |

Table 5. Initial TAWS implementation of $C_T$ algorithm

| Scene Complexity | $S_c$ (degrees C) 0 to 1 | > 1 to 2 | > 2 to 4 | > 4 |
|---|---|---|---|---|
| | $C_T$ (degrees C) | | | |
| None | .05 | .05 | .05 | .05 |
| Low | > 05 | .2 | .2 | .2 |
| Medium | .05 | .2 | .5 | .5 |
| High | .05 | .2 | .5 | 2.0 |

In operational use it was found that the step function shown in figure 3a resulted in occasional discontinuities in detection range. To mitigate this, the step function was replaced with the continuous linear functions shown in table 6 and figure 3b. Hence, in conjunction with scene complexity, the larger the temperature difference among backgrounds (i.e., the higher the scene contrast $S_C$), the higher the value of $C_T$, which in turn lowers the value of SCR ($\propto C_T^{-1}$). The lower SCR is, the fewer equivalent line pairs there are per target (see eq [7]), which effectively reduces the detection range. In general, as the number of backgrounds increases the detection range will change, generally decreasing in value somewhat. This is reasonable since by adding backgrounds, one is effectively increasing the clutter and making the target more difficult to detect. Thus, the algorithm in TAWS for determining $C_T$ is reasonable; however, the boundaries for $C_T$ and $S_C$, chosen by Schmieder [16,17] using his experience and expertise, are subject to review. As indicated in a previous paragraph for $C_T$; and as Schmieder pointed out [17] for $S_C$ "These values result from heuristic and judgmental considerations. They have not been derived from sensitivity trades, which rigorously calculate the clutter levels that are obtained from various background contrast conditions. Such a comprehensive study will be eventually needed to arrive at more fully supported values."

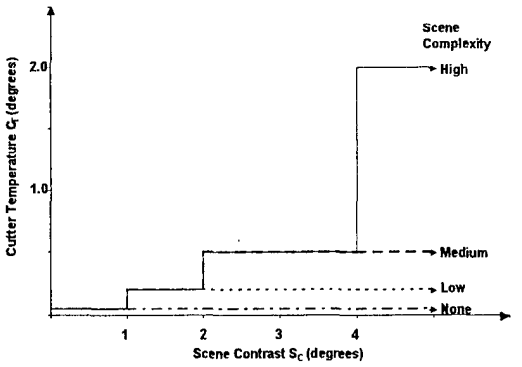


Figure 3a. Initial clutter temperature algorithm.

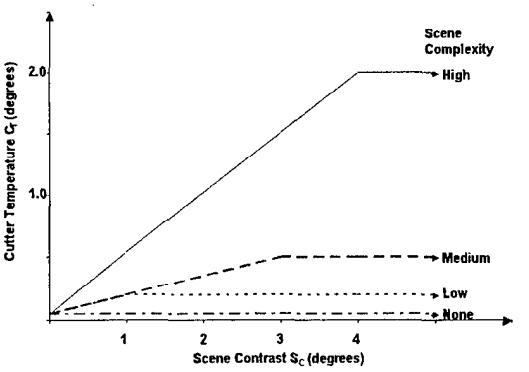


Figure 3b. Current clutter temperature algorithm.

Table 6. Current TAWS implementation of $C_T$ algorithm

| Scene complexity | $S_C$ (degrees C) 0 to 1 | >1 to 3 | >3 to 4 | >4 |
|---|---|---|---|---|
| | $C_T$ (degrees C) | | | |
| None | .05 | .05 | .05 | .05 |
| Low | .05 +0.15 $S_C$ | .2 | .2 | .2 |
| Medium | .05 +0.15 $S_C$ | | .5 | .5 |
| High | .05 +0.4875 $S_C$ | | | 2.0 |

This clutter algorithm has an unexpected effect on MRT detection ranges. When only one background is selected by the user (i.e., no scene-thermal clutter), or if the temperature difference among the selected backgrounds is ≤ 1.0, the acquisition range found is the same whether the user selected scene complexity is low or medium. Note the middle scene contrast categories now break at 3° rather than 2° for medium-scene complexity. This change is not significant since the impact on clutter temperature is at most .15°, and the original distinction between low and moderate scene contrast categories was an arbitrary selection between the threshold values of 1 for none and 4 for high.

### 2.2.3 Discussion

Johnson's paper mentioned the issue of background clutter. He emphasized that his detection criteria (1.0-line pairs) were applicable under conditions that required some degree of target shape discrimination in order to detect the target from other objects in the background, (i.e., where background clutter was present). He also stated that the number of line pairs required to attain a particular detection probability could vary significantly depending upon the nature of the background clutter. This raised a number of questions as to the significance of background clutter on the validity of the Johnson criteria, especially since Johnson did not provide a definition of clutter.

Schmieder noted that the Johnson criteria for target detection (1.0 cycles or line pairs) correlated well with his moderate-clutter category (implying that such a level of clutter was probably present in Johnson's work, although Johnson did not measure it). Comparison of Schmieder's detection probability as a function of resolution with Acquire's TTPF (see figure 4) clearly shows that Acquire's formalization compares favorably with Schmieder's moderate clutter. Other clutter levels can be accommodated in Acquire by varying $N_{50}$.

**Figure 4. Probability of detection versus [illegible]olution for 50 [illegible]t acquisition [illegible]g the TAWS [illegible] Acquire algorithms.**

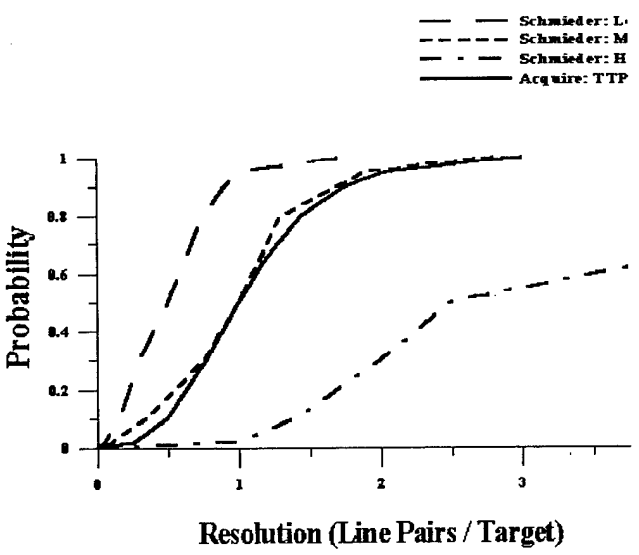

# 3. Comparisons

## 3.1 Scenarios

To compare these two complex target-acquisition models requires standardization of as many parameters as possible. To accomplish this, one weather scenario was used in conjunction with one sensor and target, both with fixed orientations.

A winter scenario was chosen and examined using an exercised T-80 Soviet main battle tank against two backgrounds (vegetation and snow) at IR wavelengths. The sensor and tank were aligned such that the sensor always had a frontal view of the tank; the sensor height was fixed at 300 ft facing north. To minimize shadow effects, the date was fixed at 21 December at a local time of 12N. The location was also fixed at latitude of 37°32' N, longitude of 127°00' E (Seoul, S. Korea). The weather conditions include (see table 7) clear skies with varying visibility and relative humidity, and overcast skies with varying visibility and relative humidity. Additional cases were run including light/heavy fog conditions, snow, drizzle, and rain.

**Table 7. Weather conditions used in the study**

| **Relative Humidity** | 30% | 50% | 80% | 100% | 100% | 80% | 90% | 90% |
|---|---|---|---|---|---|---|---|---|
| **Precipitation** | none | none | none | light fog | heavy fog | snow | light rain | moderate rain |
| **Cloud Cover** | clear | clear | clear | clear | clear | | | |
| | overcast | overcast | overcast | overcast | overcast | overcast | overcast | overcast |
| **Visibility** | 2 km | 2 | 2 | 2 | 2 | 2 | 2 | 2 |
| | 5 km | 5 | 5 | 5 | | 5 | 5 | |
| | 10 km | 10 | 10 | 10 | | 10 | 10 | |
| | 15 km | 15 | 15 | 15 | | 15 | 15 | |

## 3.2 Model Runs

The TAWS was run using winter climatology along with the weather conditions listed in table 7. Comparisons were made with the scene complexity initially set at "low." To reduce the possibility of errors, Acquire was initially run separately; however, this procedure was fraught with problems (see table 8). To alleviate this, the Acquire algorithm was programmed directly into TAWS, thereby, insuring that the many values ($\Delta T$, atmospheric transmission) were identical in both programs. Discussion on the problem and their resolution appear in table 8.

**Table 8. Problems between the TAWS and Acquire algorithms and their resolution**

| Problem | Routine | | Resolution |
|---|---|---|---|
| | TAWS | Acquire | |
| Characteristic dimension | Target height | $\sqrt{(X_{eff} * Y_{eff})}$ | Target height |
| Sensor curves | Horizontal (1D) | Horizontal and Vertical (2D) | 1D |
| Aspect ratio | $\sqrt{(7/2\ X_{eff}/Y_{eff})}$ | $\leq 3$ | $\sqrt{(7/2\ X_{eff}/Y_{eff})}$ |
| Backgrounds | 3 allowed | N/A | 1 used |
| Scene complexity | None, low, moderate, high | N/A† | Low |

† See section 3.2.5

### 3.2.1 Characteristic Dimension

The TAWS and Acquire use different target-characteristic dimensions. For MRT calculations, TAWS uses the target height; whereas, 2D Acquire uses the square root of the target's projected area as seen by the sensor. When Acquire was programmed into the TAWS, thereby using a 1D formulization, the characteristic dimension was changed to use the target height.

In the course of this study the TAWS and Acquire target T-80 Soviet main battle tank databases were examined; the results from TAWS and Acquire databases, and additional sources, are presented in table 9. The CASTFOREM is the U.S. Army's entity level warfare simulation; World Wide Web (WWW) 1, 2, and 3 were taken from various, unsubstantiated, WWW sources for comparison purposes. The values selected for the various dimension sizes probably represent different configurations of

the T-80 (cf. figures 5a and b). Using the gun-forward length is not representative of the actual target size and will produce overly optimistic detection ranges. The TAWS database has been subsequently changed to reflect the more accurate values. Once Acquire was coded into the TAWS, both algorithms used the same database.

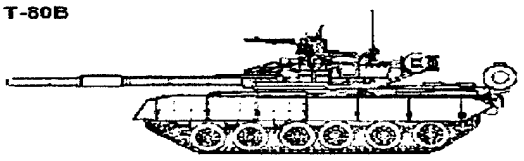


Figure 5a. T–80B

Figure 5b. T–80U

**Table 9. T-80 dimensions**

| Source | Length (m) | Width (m) | Height (m) |
|---|---|---|---|
| Acquire‡ | - | 3.59 | 2.64 |
| TAWS | 9.1 | 4.64 | 3.73 |
| CASTFOREM | 6.75 | 3.55 | 1.5** |
| WWW1 | 9.7 | 3.6 | 2.2 |
| WWW2 | 9.9/7.4§ | 3.4 | 2.2 |
| WWW3 | 7.01 | 3.6 | 2.20 |

‡ values are for projected area
§ gun forward/hull
** does not include turret

### 3.2.2 Sensor Curves

Because the TAWS was constructed during the 1980s, it uses 1D MRT curves, whereas, Acquire uses 2D MRT curves. Initially, before coding the Acquire algorithm into TAWS and the two codes were executed separately, it was necessary to ensure that the two IR sensor curves that were being used were the same. This was accomplished by multiplying the TAWS abscissa by the normalization factor of .75 (see section 2.2.1); the resulting comparison is presented in figure 6. As shown, the two sensor curves are identical. When Acquire was coded into TAWS and thus used TAWS MRT curves, N50 for detection was changed from .75, appropriate for the 2D algorithm, to 1.0, appropriate for the 1D algorithm.

**Figure 6. Comparison of the TAWS and Acquire MRT curves.**

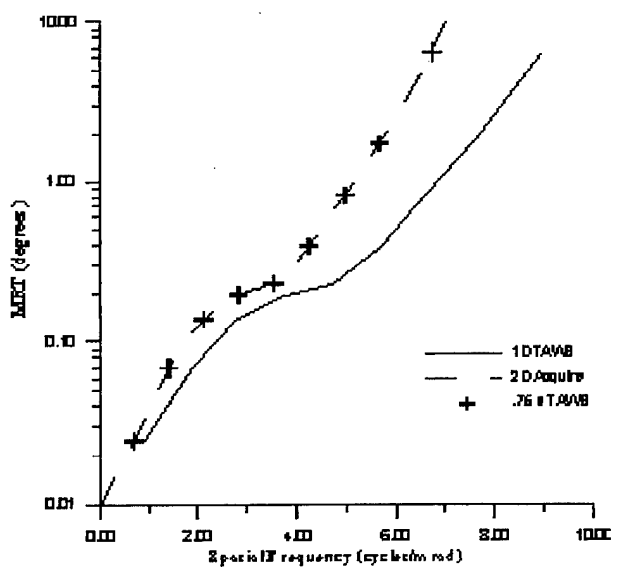


### 3.2.3 Aspect Ratios

In 1D Acquire, the target was described by its minimum dimension; thus, targets with dimensions (length x width) of 2m x 2m or 2m x 4m or 2m x 16m and identical $\Delta T$ would all be equally detectable according to 1D Acquire. The aspect ratio adjustment compensates for this unrealistic result. This is an important issue for large aspect ratio targets such as battleships but not for the typical aspect ratios of ground vehicles. In 2D Acquire, the target is described by the square root of its area; thus, the 2 m x 16 m

target will have a higher estimated probability of detection than the 2 m x 2 m target. Therefore, in moving from 1D to 2D Acquire, we have gone from the simplifying assumption that all targets of the same height are equally detectable (given the same $\Delta T$) to the simplifying assumption that all targets with the same presented area are equally detectable; however, aspect ratios > 3 are not recommended for Acquire. [3] For the typical aspect ratios of ground vehicles, this is a reasonable simplifying assumption for 2D Acquire.

When using 1D acquisition models such as TAWS, the first step conventionally performed in range prediction is to convert the laboratory MRT to take into account the scene object aspect ratio (maximum to minimum object dimension) if use is to be made of the concept that an object is more readily discerned if the aspect ratio is greater than unity. The laboratory MRT is computed or measured with a bar aspect ratio of 7. It can be shown [19] that

$$\mathrm{MRT}_{\mathrm{field}} = \mathrm{MRT}\sqrt{7/(2N\varepsilon)}, \tag{8}$$

where $\varepsilon$ is the scene aspect ratio.

For example, for detection only one cycle is required ($N = N_{50} = 1$), yielding $\mathrm{MRT}_{\mathrm{field}} = \mathrm{MRT}\sqrt{7/2\varepsilon}$. Within TAWS, the MRT is adjusted by a factor of $\sqrt{7X_{eff}/2Y_{eff}}$, where $X_{eff}$ (along-track) and $Y_{eff}$ (cross-track) are the projected target dimensions at a given range. The cross-track and along-track dimensions, viewed in a plane coincident with the sensor, are the abscissa and ordinate, respectively. Since the calculation of aspect ratio is integral to TAWS calculations, no changes were made to the algorithm.

### 3.2.4 Backgrounds

The TAWS allows calculations for scenes that include up to three backgrounds; whereas, Acquire does not consider differing backgrounds, primarily because Acquire accounts for clutter through variation of the parameter N50. The TAWS backgrounds are intimately connected with the clutter calculations (see section 2.2.2), allowing $\Delta TT$ in eq (6) to vary as the backgrounds are cycled. Thus, eq (6) can be rewritten as

$$SCR_i = \Delta T_{T_i} / \sum_{j=1}^{N_B} C_{T_j} \ , \tag{9}$$

where the subscript $i$ refers to the background under consideration (considered primary) and the subscript $j$ refers to the number of (user-entered) backgrounds $N_B$ (maximum of 3). Thus, the TAWS detection ranges for all backgrounds are calculated with the displayed background, as printed on the output, considered primary. A discussion of the lack of backgrounds in Acquire, which are intimately tied to the clutter calculations in TAWS, is deferred to the clutter section below.

### 3.2.5 Clutter

Schmieder's work, as implemented in TAWS, accounts for various levels of clutter; whereas, Acquire only accounts for clutter by varying $N_{50}$. However, as shown in section 2, Acquire's algorithm, with $N_{50}$ = 1 (detection) compares favorably with Schmieder's at moderate clutter levels. To effectively represent Schmieder's low and high clutter cases, $N_{50}$ takes on values of 0.5, and 2.5 respectively (see figure 7). Since clutter is a subjective measure, other values of $N_{50}$ may be chosen.

**Figure 7. Acquire versus the TAWS clutter comparison.**

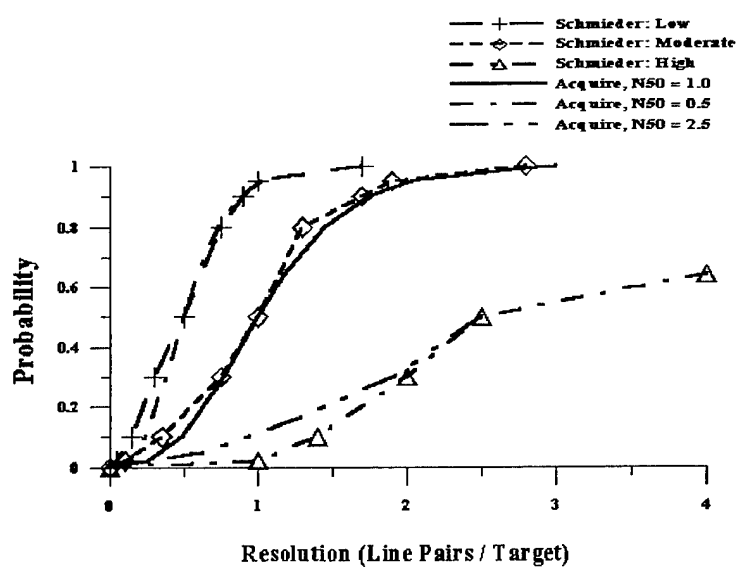

## 3.3 Results

The December 21 cases were run using low-scene complexity with a single vegetation background in TAWS, and with $N_{50}$ = 0.5 in Acquire. Results showing the detection ranges predicted at noon in each case by TAWS and Acquire are shown in figure 8.

Examination of the data shows a maximum value for the TAWS calculations at 32.1 km for the vegetation background due to sensor optical resolution limits. Because this limits scales with target height, a determination can be made using values taken from reference 18 tables A.1-2. For the sensor and target chosen the range limit turns out to be 32.8 km in good agreement with the TAWS values. This same cutoff for a maximum detection range was applied to the Acquire results.

For detection ranges less than 10 km the agreement between Acquire and TAWS was also good. Between these high and low detection ranges, i.e., midrange values between 10 and 30 km, Acquire predictions were 10 to 15 percent lower than the TAWS. Specifically, the cases with heavy fog or precipitation have identical values below 10 km, while the cases with low or moderate humidity and high visibilities have values of km. Thus, we may draw the conclusion that the contribution from approximately 32 clutter is irrelevant in instances when the weather conditions are either extremely unfavorable (low visibility) or extremely favorable (high visibility).

**Figure 8. The ; versus ire-detection ges at 50 percent probability of detection.**

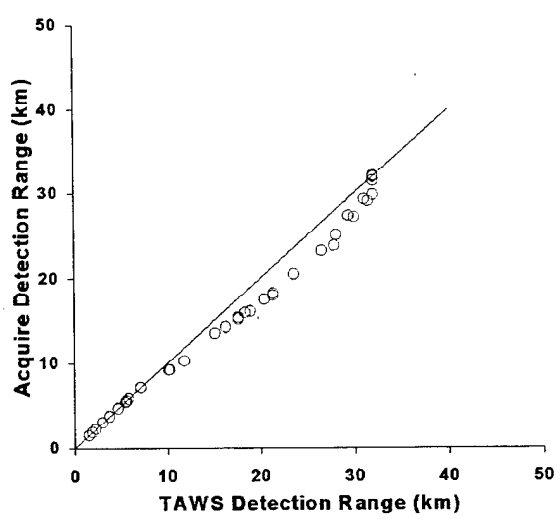

Some of the discrepancy between the TAWS and Acquire in the midrange may be explained by the fact that the clutter temperature in the TAWS runs with one background and low-scene complexity is 0.125 °C (tables 4 and 6), which equates to an $N_{50}$ value of approximately .3, while the value used for these Acquire runs ($N_{50}$ = 0.5) could be associated with a low-clutter value of 0.2 °C. However, note that Acquire does not use clutter temperature directly. Increasing the clutter temperature to 0.2 °C in the TAWS, by including an additional background with an appropriate scene contrast temperature, did lower the TAWS range but only accounted for less than half of the discrepancy between the TAWS and Acquire values. When additional Acquire runs were made with $N_{50}$ set = .3, which is not strictly analogous to calculating a clutter level in TAWS, the results were within 5 percent of the TAWS values.

### 3.3.1 Clutter/Complexity Effects

Because the user can select a scene complexity level of none, low, moderate, or high in the TAWS (specified as Clutter/Complexity in the User Interface), it is important to understand how this selection affects the resulting detection range. Only one background was used for these comparisons in order to hold constant the scene contrast component of clutter. These comparisons showing the effects of the choice of scene complexity in TAWS include the complete hourly data from the December 21 runs, rather than just the noontime data. The standard deviations of the difference between TAWS and Acquire detection ranges throughout each daily run are small, indicating that diurnal variations behave similarly in both TAWS and Acquire. In general, most cases using one background displayed a decrease in detection range of approximately 5 percent when scene complexity was increased from none to low or moderate, and another 5 percent decrease when scene complexity was increased from low or moderate to high. However, there is a fair amount of variation from this typical result, as shown by the sample of runs plotted in figure 9. In this figure, the abscissa represents the cases run (generally in order of cases with low humidity on the left to cases with high humidity and precipitation on the right), and the ordinate showing the percent of the resulting detection range with a given level of scene complexity compared to the range found with scene complexity set to none. Note from tables 4 and 6 that with only one background low- and moderate-scene complexity will return the same values.

Figure 9. Scene complexity effects on target- detection ranges.

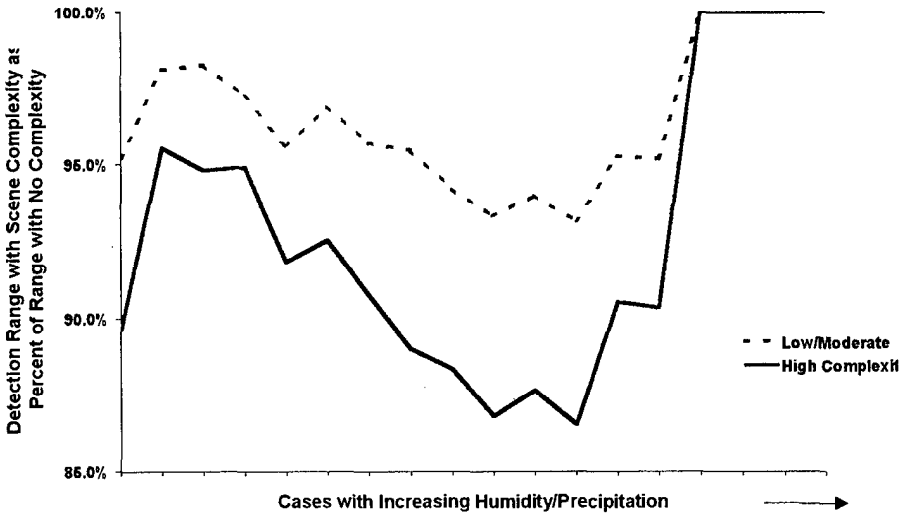


The primary exception to the general impact of varying scene complexity occurs both when TAWS detection ranges are very long and when they are very short. For example, results plotted toward the left side of figure 9 include cases where humidity is 50 percent or less, and there is no fog or precipitation. These conditions result in long detection ranges, which are not substantially decreased when the scene complexity level is increased. Additionally, cases plotted on the right side of the graph provide very short detection ranges due to fog or precipitation; so that increasing the complexity level has no corresponding decrease in detection range, since the detection range is already so restricted. Other deviations are related to the selected visibility in each case, with increasing scene complexity causing impacts more than the usual 5 percent when visibility is great. In order to highlight the general trend, cases with visibilities of 2 and 15 km have been omitted from figure 9, which would otherwise show even greater fluctuations. The cases potted with visibilities of 5 and 10 km reflect some fluctuation related to whether the cloud cover was entered as clear or overcast, which accounts for the up-and-down nature of the graph.

Another result occurs when multiple backgrounds are selected in the TAWS. The previous results were based on cases using vegetation as the only background. If a second background is added, it affects the detection range predicted for the first background if the complexity level is set to anything other than none. The effect of adding a second background is shown in table 10, using the noontime values and excluding the cases reflecting extreme high or low detection ranges. As

expected, detection ranges for the vegetation background decrease when the second background of snow is added, since the clutter has been increased. Additionally, detection ranges for the vegetation background increase when snow is entered as the primary background with vegetation as the secondary background. This is expected because the thermal contrast ($\Delta T$) between the target and the background is calculated using the first, or primary, background entered in TAWS; the secondary background does not interact with the target. Because snow has a higher albedo than the vegetation, a relatively greater amount of the solar radiation is reflected onto the tank surface raising its temperature; and, thus, producing the larger contrast value.

**Table 10. Impact of a second background on detection range**

| | TAWS Range (km) | | |
|---|---|---|---|
| **Scene complexity** | **Vegetation background only** | **Vegetation background primary with snow background secondary** | **Vegetation background secondary with snow background primary** |
| None | 22.46 | 22.46 | 23.30 |
| Low | 21.46 | 21.36 | 22.22 |
| Moderate | 21.46 | 21.07 | 21.95 |
| High | 20.39 | 19.87 | 20.81 |

As discussed in section 2.2.2, rather than a second choice of a background for a *what if* capability to see two separate background results in a single model run, adding a second background serves to add clutter to the scene, with the greatest impact in conjunction with the selection of moderate-or-high complexity. Note that when multiple backgrounds are selected, there can be a difference between detection ranges based on low and moderate complexity, as well as even greater differences between moderate and high complexity than seen with just one background. This is a reasonable result, and has been highlighted in the updated TAWS user documentation (Version 2.1 and greater). In cases with multiple backgrounds, the clutter temperature $C_T$ will not necessarily be consistent for each time in a 24-hour run, or between cases with varying weather input, due to the differential heating of the target and the different background types. However, to get an idea of the total effects possible under different clutter amounts, a single example at a single time shows a

decrease in detection range from 19.69 km based on a single background and no scene complexity to 15.75 km based on three backgrounds and high-scene complexity.

#### 3.3.2.2 Weather Effects

Although one purpose of this report is to compare the predicted target-detection ranges output by the TAWS and Acquire, it is also worth examining the effects of weather on the predicted ranges. Varying visibility, relative humidity, cloud cover, fog, and precipitation resulted in similar impacts to detection ranges in both the TAWS and Acquire, consistent with at least qualitative expectations of how these atmospheric properties affect IR sensors. [20,21]

The following examples are based on fairly realistic winter-weather scenarios for Seoul, Korea. Climatological temperature values varied 6 °C over the 24-hr period, with less variation in dew-point temperature values, resulting in a typical increase in relative humidity values in the early morning and lower relative humidity in the afternoon. These same temperature values were used whether or not clouds, fog, or precipitation were included. These examples are based on low-scene complexity and one background in the TAWS, and $N_{50}$ = 0.5 in Acquire. As discussed above, increasing the complexity level to high provided somewhat shorter detection ranges in most cases, but yielded similar results in terms of weather impacts on detection-range predictions. Table 11 lists the noontime detection ranges calculated by the TAWS (number in upper left of cell) and Acquire (number in lower right of cell) for each weather scenario. As previously discussed, the Acquire values are not resolution limited to the TAWS' appropriate maximum of 32 km in cases with high visibility and no fog or precipitation. Other cases, which include fog or precipitation seem to return detection ranges around 7 km using Acquire, while the TAWS provides much lower detection ranges. Otherwise, Acquire results show similar impacts based on weather and diurnal effects as the TAWS, and subsequent discussions will highlight the specific-weather impacts using the TAWS data.

Table 11. Detection ranges as a function of various weather scenarios

| Detection Ranges (km) TAWS Acquire | | | | | | | | | | | | | | | | | |
|---|---|---|---|---|---|---|---|---|---|---|---|---|---|---|---|---|---|
| RH Precipitation | | 30 % none | | 50 % none | | 80 % none | | 100 % light fog | | 100% heavy fog | | 80 % snow | | 90% light rain | | 90% moderate rain | |
| Cloud Cover | | clear | overcast | clear | overcast | clear | overcast | clear | overcast | clear | overcast | clear | overcast | clear | overcast | clear | overcast |
| Visibility (km) | 2 | 21 | 18 | 20 | 18 | 19 | 16 | 5 | 5 | 2 | 2 | | 2 | | 5 | | 3 |
| | | 18 | 16 | 17 | 15 | 16 | 14 | 5 | 5 | 2 | 2 | | 2 | | 5 | | 3 |
| | 5 | 32 | 28 | 30 | 27 | 28 | 24 | 12 | 10 | | | | 4 | | 5 | | |
| | | 29 | 25 | 27 | 23 | 24 | 20 | 10 | 9 | | | | 4 | | 5 | | |
| | 10 | 32 | 32 | 32 | 31 | 32 | 28 | 18 | 15 | | | | 7 | | 6 | | |
| | | 32 | 32 | 32 | 29 | 30 | 25 | 15 | 14 | | | | 7 | | 6 | | |
| | 15 | 32 | 32 | 32 | 32 | 32 | 29 | 21 | 18 | | | | 10 | | 6 | | |
| | | 32 | 32 | 32 | 32 | 32 | 27 | 18 | 16 | | | | 9 | | 6 | | |

3.3.2.1 Visibility

Although IR sensors are useful for detecting targets at ranges beyond the distance visible to the unaided eye, the same atmospheric constituents, which reduce visibility, will reduce IR detection ranges, although to a different amount. Figure 10 illustrates the impact of reduced visibility on TAWS. Under the benign conditions of low-relative humidity (around 30 percent at noon), clear skies, and 15 km visibility, TAWS provides a maximum sensor-detection range limit of 32 km throughout the 24-hour period. The other examples with clear skies result in an increase in detection ranges during daylight hours, as solar loading heats the target more than the background, resulting in a greater $\Delta T$ (or differential in target/background temperatures). Visibility decreasing from 15 to 10 km generates minimal impacts, but going from 10 to 5 km causes a 15 percent decrease in detection range, while going from 5 to 2 km results in a 35 percent decrease.

Figure 10. Visibility impacts on the TAWS-detection ranges.

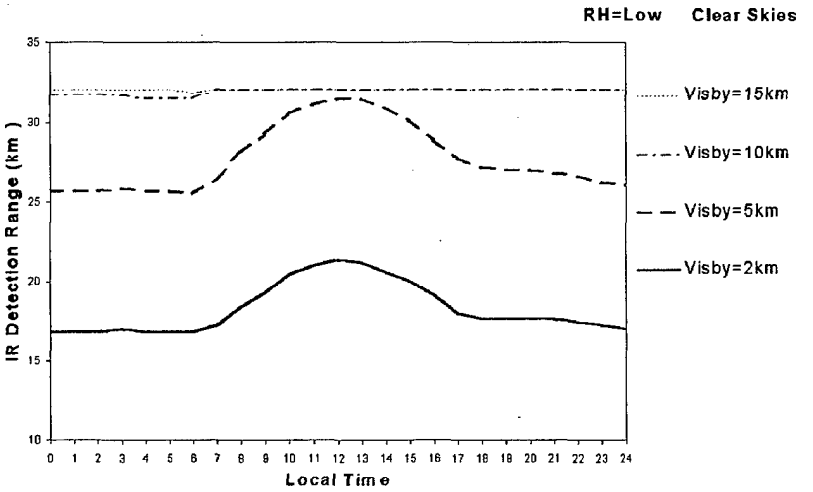


3.3.2.2 Relative Humidity

Atmospheric moisture absorbs IR signals. Because the time series of temperature values is consistent in each case, changing the relative humidity is equivalent to changing the amount of water vapor or absolute humidity available for attenuation of the sensor signal. Figure 11 shows an example of increasing humidity resulting in decreasing detection ranges. Since the cold winter temperatures used in these cases do not allow the atmosphere to contain significantly more moisture, the detection range is only decreased by 10 percent as humidity is varied from low (approximately 30 percent; equivalent to 2 g/m$^3$) to high (approximately 80 percent; equivalent to 4 g/m$^3$). However, comparable runs made using summer temperatures show noon-time detection range predictions of 28 km in low humidity (approximately 30 percent; equivalent to 7 g/m$^3$) falling to 13 km in high humidity (approximately 80 percent; equivalent to 19 g/m$^3$), reflecting more than a 50 percent decrease.

Figure 11.
Relative humidity impacts on the TAWS-detection ranges.

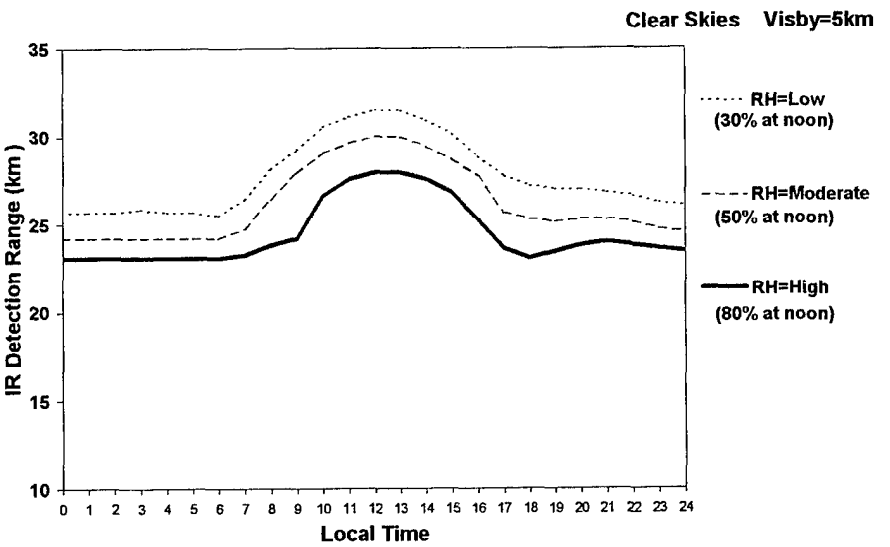


3.3.2.3 Sky Cover

The primary effect of cloud cover above the sensor path is based on the cloud's influence on heating and cooling of the target and the background. As shown in figure 12, this example exhibits slightly longer detection ranges during the night with overcast skies compared to clear skies. Although both the target and the background temperatures are affected by the clouds, so that the $\Delta T$ remains smaller than when no clouds are present, less radiational cooling allows the thermal imager to detect the warmer target at slightly longer ranges than under clear skies. Cloud cover has a greater impact during the day, as the reduced solar loading provides only a 5 percent detection range increase, while the case with no clouds produces a twenty percent greater detection range during the daytime.

Figure 12. Sky cover impacts on the TAWS-detection ranges.

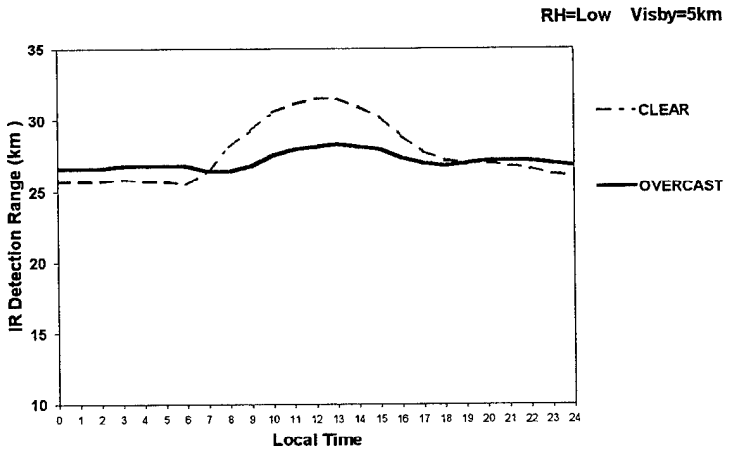


3.3.2.4 Fog and Precipitation

The type, size, and number of atmospheric particles associated with fog and precipitation significantly attenuate target acquisition sensor signals. Figures 13 and 14 display different Y-axis values than preceding charts, reflecting the substantially reduced detection ranges predicted under conditions of fog or precipitation. Although radiative fog is generally not associated with overcast conditions, total sky cover has been used to provide consistency in comparing results. These cases show no diurnal variation in detection ranges, since the target and background heating and cooling cycles are dampened by the liquid water in the atmosphere. The TAWS provides detection ranges of approximately 4.5 km for both the light/radiation fog and light-rain cases. Compared to light fog or rain, the TAWS reflects approximately 40 percent decrease in detection range for moderate rain, 60 percent decrease for heavy/advection fog, and 65 percent decrease for snow.

Figure 13. Fog impacts on the TAWS-detection ranges.

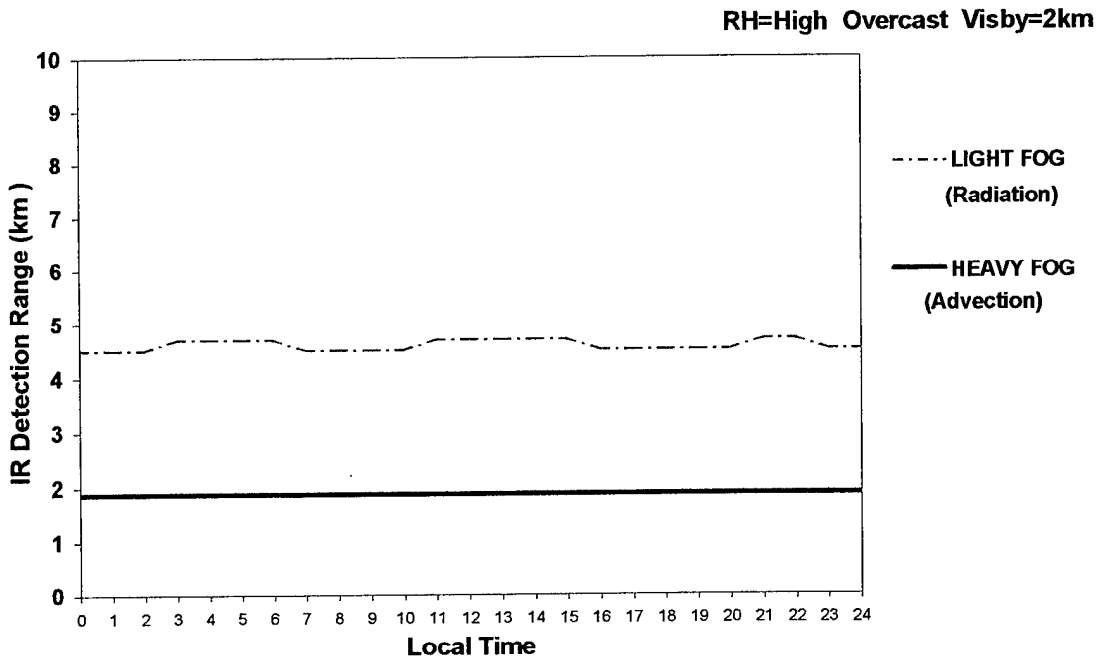


Figure 14. Precipitation impacts on the TAWS-detection ranges.

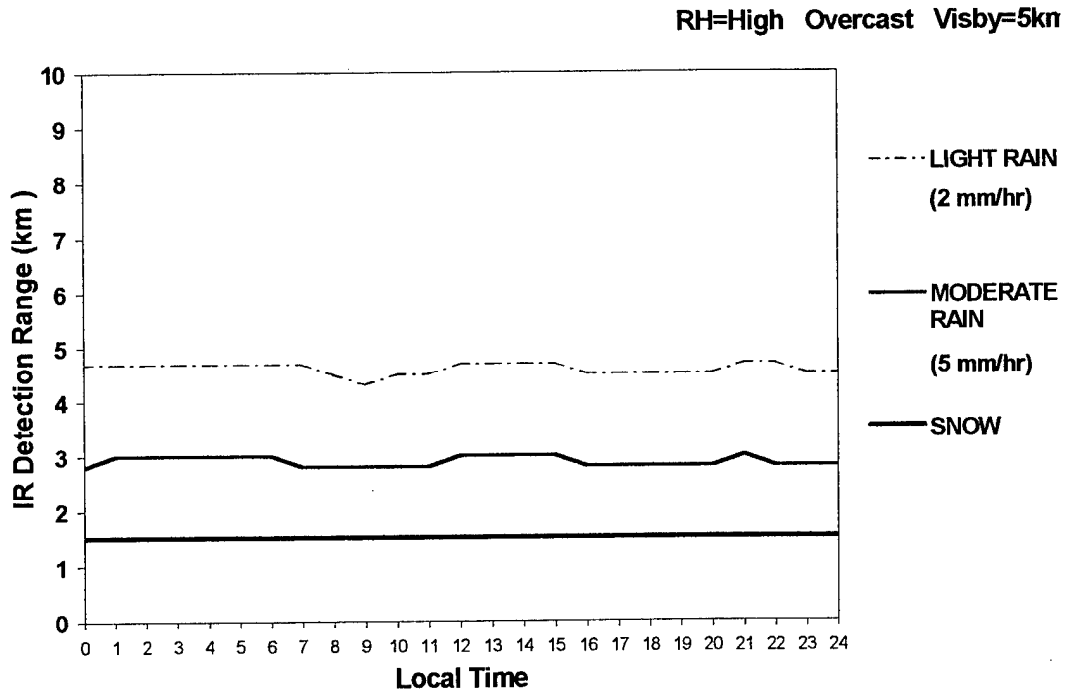

# 4. Conclusions

It is important that Acquire be merged into the TAWS so that the services can predict target acquisition of ground targets using recognition and identification in addition to detection. The incorporation of the Acquire SPM into the TAWS is scheduled for the TAWS Version 3, which will be released for use in 2001. These comparisons of the target-acquisition range output from the current version of the TAWS with output from Acquire provide positive feedback on the benefits of this enhancement to the TAWS, while maintaining the existing interfaces and providing comparable target-detection range predictions. The primary benefit of this enhancement will be the ability to specify target-acquisition discrimination levels, including detection, recognition, and identification. Decisions will need to be made on an efficient and appropriate selection of $N_{50}$ for use in the Acquire SPM.

Because the cases examined in this report are limited to a winter scenario in Korea, specific quantitative results of the selected weather parameters' impacts on target-detection range cannot be generalized to all situations. However, these cases do highlight the importance of considering accurate atmospheric conditions in target-acquisition predictions. Results showing a smaller weather impact to Acquire-detection ranges than predicted using the current TAWS SPM under conditions of fog or precipitation warrant additional investigation.

## References


1. Sauter, D., M. Torres, J.D. Brandt, et al., "The Integrated Weather Effects Decision Aid: A Common Software Tool to Assist in Command and Control Decision Making," *Proceedings of the Command & Control Research & Technology Symposium,* Newport, RI, (June 1999).

2. Gouveia M.J., J.S. Morrison, R.B. Bensinger, et al., "TAWS and NOWS: Software Products for Operational Weather Support," *Proceedings of the Battlespace Atmospheric and Cloud Impacts on Military Operations Conference,* Colorado State University, Fort Collins, Colorado, (25-27 April 2000).

3. *Acquire Range Performance Model for Target Acquisition Systems,* Version 1 User's Guide, U.S. Army CECOM Night Vision and Electronic Sensors Directorate Report, Ft. Belvoir, VA, (1995).

4. Johnson, J., "Analysis of Image Forming Systems," *Proceedings of the Image Intensifier Symposium,* U.S. Army Engineer Research and Development Laboratory, Ft. Belvoir, (AD 220 160), (October 1958).

5. Schmieder, D.E., and M.R. Weathersby, *Detection Performance in Clutter with Variable Resolution,* IEEE Transactions on Aerospace and Electronic Systems, Version 19, pp. 622-630, (July 1983).

6. Schmieder, D.E., M.R. Weathersby, W.M. Finlay, et al., *Clutter and Resolution Effects on Observer Static Detection Performance,* U.S. Air Force Wright Aeronautical Laboratory, Technical Report AFWAL-TR-82-1059 (AD B071777), Wright-Patterson AFB, OH, (June 1982).

7. Touart, C.N., M.J. Gouveia, D.A. DeBenedictis, et al., *Electro-Optical Tactical Decision Aid (EOTDA) User's Manual,* Version 3, Technical Description, U.S. Air Force Phillips Laboratory, Technical Report PL-TR-93-2002 (AD B172088L), Hanscom AFB, MA, (June 1994).

8. *Army Modeling and Simulation Office,* Standards Category Acquire, web site, http://www.amso.army.mil/.

9. Johnson, J., and W.R. Lawson, "Performance Modeling Methods and Problems," *Proceedings of the IRIS Specialty Group on Imaging,* pp. 105-123, Infrared Information and Analysis Center, ERIM, Ann Arbor, MI, (January 1974).

10. Mazz, J., "Acquire Model: Variability in N50 Analysis," *Proceedings 9th Annual Ground Target Modeling and Validation Conference,* Signature Research, Inc., Calumet, MI, (August 1998)

11. Howe, J.D., *Electro-Optical Imaging System Performance Prediction, in The Infrared and Electro-Optical Systems Handbook* (U), volume 4., M.C. Dudzik, Ed, Infrared Information Analysis Center and SPIE Optical Engineering Press, (1993).

12. Berk, A., L.S. Bernstein and D. C. Robertson, *MODTRAN: A Moderate Resolution Model for LOWTRAN 7*, U.S. Air Force Geophysics Laboratory, Technical Report, GL-TR-89-0122 (AD A214337), Hanscom AFB, MA, (1989).

13. Shirkey, R.C., L.D. Duncan and F.E. Niles, *The Electro-Optical Systems Atmospheric Effects Library*, Executive Summary, Atmospheric Sciences Laboratory, Technical Report, ASL-TR-0221-1, White Sands Missile Range, NM, (October 1987).

14. Higgins, G.J., P.F. Hilton, R. Shapiro, et al., *Operational Tactical Decision Aids (OTDA)s* , U.S. Air Force Geophysical Laboratory, Technical Report, GL-TR-89-0095 (AD B145 289), Hanscom AFB, MA, (March 1989).

15. Higgins, G., D.A. DeBenedictis, M.J. Gouveia, et al., *Electro-Optical Tactical Decision Aid (EOTDA) Final Report*, U.S. Air Force Geophysics Laboratory, Technical Report, GL-TR-90-0251 (I) (AD B153311L), Hanscom AFB, MA, (September 1990).

16. Schmieder, D.E., *Technique for Incorporating High Resolution Target Signature Predictions into Sensor Performance Models*, U.S. Air Force Wright Aeronautical Laboratory, Technical Report, AFWAL-TR- 87-1055, Wright-Patterson AFB, OH, (July 1987).

17. Schmieder, D.E., *Interim Contrast Categories for 'Rule of Thumb' Clutter Computation*, Georgia Technical Research Institute, Technical Transmittal, TT-4828-004, Atlanta, GA, (March 1988).

18. Touart, C.N., M.J. Gouveia, D.A. DeBenedictis, et al., *Electro-Optical Tactical Decision Aid (EOTDA) User's Manual*, Version 3, Technical Description, Appendix A, Phillips Laboratory Technical Report PL-TR-93-2002 (II) (AD B171600L), Hanscom AFB, MA, (January 1993).

19. Holst, G.C., *Electro-Optical Imaging System Performance*, JCD Publishing, Winter Park, FL, (1995).

20. *Quantitative Description of Obscuration Factors for Electro-Optical and Millimeter Wave Systems*, Military Handbook, DOD-HDBK-178(ER), (July 1986).

21. Federation of American Scientists, *METOC Effects Smart Book* (U), web site, http://www.fas.org/spp/military/program/met/metocsmarttbook.htm

## Acronyms

| | |
|---|---|
| 1D | one dimensional |
| 2D | two dimensional |
| AMSAA | Army Materiel Systems Analysis Agency |
| AFRL | U.S. Air Force Research Laboratory |
| CASTFOREM | Combined Arms and Support Taskforce Evaluation Model |
| EOTDA | Electro-Optical Tactical Decision Aid |
| ERDL | U.S. Army Engineer Research and Development Laboratories |
| FLIR | forward-looking infrared |
| GTRI | Georgia Tech Research Institute |
| IFOV | instantaneous field of view |
| IWEDA | Integrated Weather Effects Decision Aid |
| IR | infrared |
| MDT | minimum detectable temperature |
| MRC | minimum resolvable contrast |
| MRT | minimum resolvable temperature |
| NVESD | Night Vision and Electronic Sensors Directorate |
| SCR | signal-to-clutter ratio |
| SPM | Sensor Performance Model |
| TASC | The Analytic Sciences Corporation |
| TAWS | Target Acquisition Weather Software |
| TCM2 | Target Contrast Model 2 |
| TDA | tactical decision aid |
| TRAC | TRADOC Analysis Center |

| | |
|---|---|
| TRADOC | Training and Doctrine Command |
| TTPF | Target Transform Probability Function |
| WWW | World Wide Web |

# Distribution

| | Copies |
|---|---|
| NASA MARSHALL SPACE FLT CTR<br>ATMOSPHERIC SCIENCES DIV<br>ATTN DR FICHTL<br>HUNTSVILLE AL 35802 | 1 |
| NASA SPACE FLT CTR<br>ATMOSPHERIC SCIENCES DIV<br>CODE ED 41 1<br>HUNTSVILLE AL 35812 | 1 |
| US ARMY STRAT DEFNS CMND<br>CSSD SL L<br>ATTN DR LILLY<br>PO BOX 1500<br>HUNTSVILLE AL 35807-3801 | 1 |
| US ARMY MISSILE CMND<br>AMSMI RD AC AD<br>ATTN DR PETERSON<br>REDSTONE ARSENAL AL 35898-5242 | 1 |
| US ARMY MISSILE CMND<br>AMSMI RD AS SS<br>ATTN MR H F ANDERSON<br>REDSTONE ARSENAL AL 35898-5253 | 1 |
| US ARMY MISSILE CMND<br>AMSMI RD AS SS<br>ATTN MR B WILLIAMS<br>REDSTONE ARSENAL AL 35898-5253 | 1 |
| US ARMY MISSILE CMND<br>AMSMI RD DE SE<br>ATTN MR GORDON LILL JR<br>REDSTONE ARSENAL AL 35898-5245 | 1 |
| US ARMY MISSILE CMND<br>REDSTONE SCI INFO CTR<br>AMSMI RD CS R DOC<br>REDSTONE ARSENAL AL 35898-5241 | 1 |
| US ARMY MISSILE CMND<br>AMSMI<br>REDSTONE ARSENAL AL 35898-5253 | 1 |

| | |
|---|---|
| PACIFIC MISSILE TEST CTR<br>GEOPHYSICS DIV<br>ATTN CODE 3250<br>POINT MUGU CA 93042-5000 | 1 |
| NAVAL OCEAN SYST CTR<br>CODE 54<br>ATTN DR RICHTER<br>SAN DIEGO CA 52152-5000 | 1 |
| METEOROLOGIST IN CHARGE<br>KWAJALEIN MISSILE RANGE<br>PO BOX 67<br>APO SAN FRANCISCO CA 96555 | 1 |
| DEPT OF COMMERCE CTR<br>MOUNTAIN ADMINISTRATION<br>SPPRT CTR LIBRARY R 51<br>325 S BROADWAY<br>BOULDER CO 80303 | 1 |
| NCAR LIBRARY SERIALS<br>NATL CTR FOR ATMOS RSCH<br>PO BOX 3000<br>BOULDER CO 80307-3000 | 1 |
| DAMI POI<br>WASHINGTON DC 20310-1067 | 1 |
| LEANDER PAGE<br>DAMI POB<br>WASHINGTON DC 20310-1067 | 1 |
| MIL ASST FOR ENV SCI OFC<br>OF THE UNDERSEC OF DEFNS<br>FOR RSCH & ENGR R&AT E LS<br>PENTAGON ROOM 3D129<br>WASHINGTON DC 20301-3080 | 1 |
| US ARMY INFANTRY<br>ATSH CD CS OR<br>ATTN DR E DUTOIT<br>FT BENNING GA 30905-5090 | 1 |
| AIR WEATHER SERVICE<br>TECH LIBRARY FL4414 3<br>SCOTT AFB IL 62225-5458 | 1 |
| USAFETAC DNE<br>ATTN MR GLAUBER<br>SCOTT AFB IL 62225-5008 | 1 |

| | |
|---|---|
| HQ AFWA/DNX<br>106 PEACEKEEPER DR STE 2N3<br>OFFUTT AFB NE 68113-4039 | 1 |
| PAUL TATTELMAN<br>AFRL VSBE<br>29 RANDOLPH ROAD<br>HANSCOM AFB MA 01731-3010 | 6 |
| DR ANDY GOROCH<br>NAVAL RESEARCH LABORATORY<br>MARINE METEOROLOGY DIV CODE 7543<br>MONTEREY CA 93943-5006 | 6 |
| MELANIE GOUVEIA<br>TASC<br>55 WALKERS BROOK DR<br>READING MA 01867 | 6 |
| US ARMY MATERIEL SYST<br>ANALYSIS ACTIVITY<br>AMXSY<br>ATTN MR J MAZZ<br>APG MD 21005-5071 | 1 |
| US ARMY MATERIEL SYST<br>ANALYSIS ACTIVITY<br>AMXSY AT<br>ATTN MS R KISTNER<br>APG MD 21005-5071 | 1 |
| US ARMY MATERIEL SYST<br>ANALYSIS ACTIVITY<br>AMSXY<br>APG MD 21005-5071 | 1 |
| US ARMY RESEARCH LABORATORY<br>AMSRL D<br>2800 POWDER MILL ROAD<br>ADELPHI MD 20783-1145 | 1 |
| US ARMY RESEARCH LABORATORY<br>AMSRL OP CI SD TL<br>2800 POWDER MILL ROAD<br>ADELPHI MD 20783-1145 | 1 |
| US ARMY RESEARCH LABORATORY<br>AMSRL SS SH<br>ATTN DR SZTANKAY<br>2800 POWDER MILL ROAD<br>ADELPHI MD 20783-1145 | 1 |

| | |
|---|---|
| US ARMY RESEARCH LABORATORY<br>AMSRL IS<br>ATTN J GANTT<br>2800 POWDER MILL ROAD<br>ADELPHI MD 20783-1197 | 1 |
| US ARMY RESEARCH LABORATORY<br>AMSRL<br>2800 POWDER MILL ROAD<br>ADLEPHI MD 20783-1145 | 1 |
| NATIONAL SECURITY AGCY W21<br>ATTN DR LONGBOTHUM<br>9800 SAVAGE ROAD<br>FT GEORGE G MEADE MD 20755-6000 | 1 |
| ARMY RSRC OFC<br>ATTN AMXRO GS DR BACH<br>PO BOX 12211<br>RTP NC 27009 | 1 |
| DR JERRY DAVIS<br>NCSU<br>PO BOX 8208<br>RALEIGH NC 27650-8208 | 1 |
| US ARMY CECRL<br>CECRL GP<br>ATTN DR DETSCH<br>HANOVER NH 03755-1290 | 1 |
| US ARMY ARDEC<br>SMCAR IMI I BLDG 59<br>DOVER NJ 07806-5000 | 1 |
| US ARMY COMMUNICATIONS<br>ELECTR CTR FOR EW RSTA<br>AMSRL EW D<br>FT MONMOUTH NJ 07703-5303 | 1 |
| US ARMY COMMUNICATIONS<br>ELECTR CTR FOR EW RSTA<br>AMSRL EW MD<br>FT MONMOUTH NJ 07703-5303 | 1 |
| US ARMY DUGWAY PROVING GRD<br>STEDP MT DA L 3<br>DUGWAY UT 84022-5000 | 1 |
| US ARMY DUGWAY PROVING GRD<br>STEDP MT M<br>ATTN MR BOWERS<br>DUGWAY UT 84022-5000 | 1 |

| | |
|---|---|
| DEPT OF THE AIR FORCE<br>OL A 2D WEATHER SQUAD MAC<br>HOLLOMAN AFB NM 88330-5000 | 1 |
| PL WE<br>KIRTLAND AFB NM 87118-6008 | 1 |
| USAF ROME LAB TECH<br>CORRIDOR W STE 262 RL SUL<br>26 ELECTR PKWY BLD 106<br>GRIFFISS AFB NY 13441-4514 | 1 |
| AFMC DOW<br>WRIGHT PATTERSON AFB OH 45433-5000 | 1 |
| US ARMY FIELD ARTILLERY SCHOOL<br>ATSF TSM TA<br>FT SILL OK 73503-5600 | 1 |
| US ARMY FOREIGN SCI TECH CTR<br>CM<br>220 7TH STREET NE<br>CHARLOTTESVILLE VA 22448-5000 | 1 |
| NAVAL SURFACE WEAPONS CTR<br>CODE G63<br>DAHLGREN VA 22448-5000 | 1 |
| US ARMY OEC<br>CSTE EFS<br>PARK CENTER IV<br>4501 FORD AVE<br>ALEXANDRIA VA 22302-1458 | 1 |
| US ARMY CORPS OF ENGRS<br>ENGR TOPOGRAPHICS LAB<br>ETL GS LB<br>FT BELVOIR VA 22060 | 1 |
| US ARMY TOPO ENGR CTR<br>CETEC ZC 1<br>FT BELVOIR VA 22060-5546 | 1 |
| US ARMY NUCLEAR CML AGCY<br>MONA ZB BLDG 2073<br>SPRINGFIELD VA 22150-3198 | 1 |
| US ATRADOC<br>ATCD FA<br>FT MONROE VA 23651-5170 | 1 |

| | |
|---|---|
| US ARMY TRADOC ANALYSIS CTR<br>ATRC WSS R<br>WSMR NM 88002-5502 | 1 |
| DTIC<br>8725 JOHN J KINGMAN RD<br>STE 0944<br>FT BELVOIR VA 22060-6218 | 1 |
| US ARMY MISSILE CMND<br>AMSMI<br>REDSTONE ARSENAL AL 35898-5243 | 1 |
| US ARMY DUGWAY PROVING GRD<br>STEDP3<br>DUGWAY UT 84022-5000 | 1 |
| WSMR TECH LIBRARY BR<br>STEWS IM IT<br>WSMR NM 88002 | 1 |
| US MILITARY ACADEMY<br>DEPT OF MATHEMATICAL SCIENCES<br>ATTN MDN A MAJ DON ENGEN<br>THAYER HALL<br>WEST POINT NY 10996-1786 | 1 |
| ARMY MODELING & SIMULATION OFFICE<br>DDCSOPS<br>ATTN DAMO ZS<br>400 ARMY PENTAGON<br>WASHINGTON DC 20310-0450 | 1 |
| US ARMY RESEARCH LABORATORY<br>AMSRL CI EW<br>ATTN DR SHIRKEY<br>INFO SCI & TECH DIR<br>WSMR NM 88002-5501 | 6 |
| US ARMY RESEARCH LABORATORY<br>AMSRL CI EW<br>ATTN B SAUTER<br>INFO SCI & TECH DIR<br>WSMR NM 88002-5501 | 6 |
| MR RENE CORMIER<br>AFRL VSBL DRC<br>29 RANDOLPH ROAD<br>HANSCOM AFB MA 01731-3010 | 6 |

| | |
|---|---|
| MR D DIXON<br>TRAC<br>ATTN ATRC WBC<br>WSMR NM 88002 | 1 |
| Record Copy | 1 |
| TOTAL | 95 |